U.S. DEPARTMENT OF ENERGY | Office of Science

NSTX-U

Study of Ion and Electron Scale Turbulence in an NSTX H-mode Plasma Using a Synthetic High-k Diagnostic and Gyrokinetic Simulation

J. Ruiz Ruiz[1]
Y. Ren[2], W. Guttenfelder[2], A. E. White[1], S.M. Kaye[2], B. P. LeBlanc[2], E. Mazzucato[2], K.C. Lee[3], C.W. Domier[4], D. R. Smith[5], H. Yuh[6]
1. MIT 2. PPPL 3. NFRI 4. UC Davis 5. U Wisconsin 6. Nova Photonics, Inc.

58th Annual Meeting of the APS Division of Plasma Physics
October 31-November 4, 2016, San Jose, California

Alcator C-Mod

PPPL

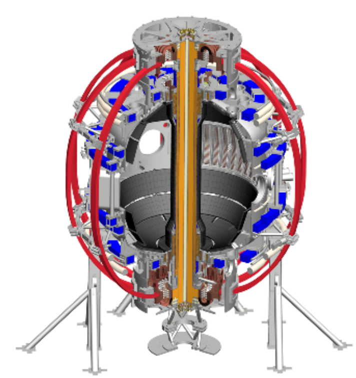

Past Work on NSTX H-mode Plasma Showed Stabilization of e- scale Turbulence by Density Gradient

- NSTX NBI heated H-mode featured a controlled current ramp-down. Shot 141767.

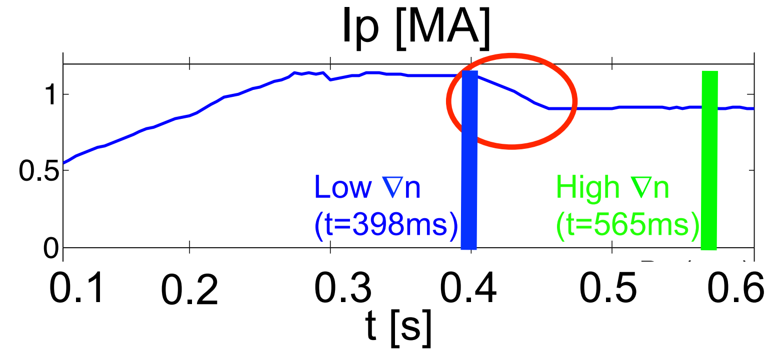

- An increase in the equilibrium density gradient was correlated to a decrease in high-k density fluctuation amplitude (measured by a high-k scattering system). *cf.* Ruiz Ruiz PoP 2015.

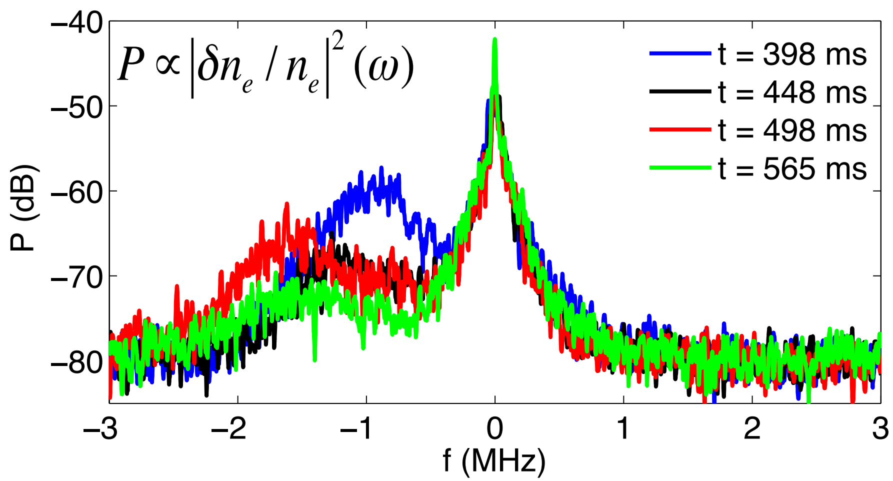

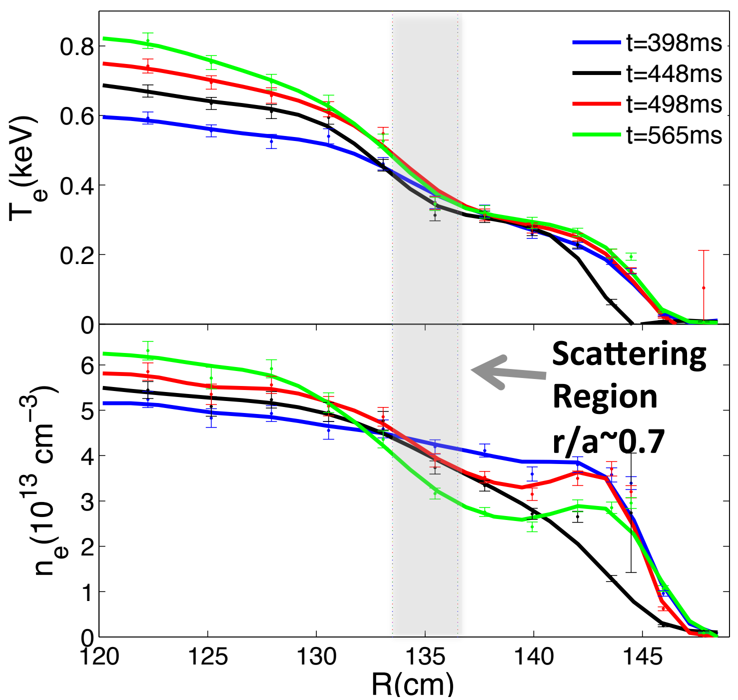

Experiment, Linear and Nonlinear Gyrokinetic Simulation Showed Density Gradient Stabilization of e- scale Turbulence

- Experimental k-spectrum is measured with a high-k scattering diagnostic (*cf.* Smith RSI 2008).
- Peak amplitude in experimental k-spectra, linear growth rate and nonlinear electron heat flux using gyrokinetic simulation is reduced, and shifted to higher wavenumber with increasing density gradient.

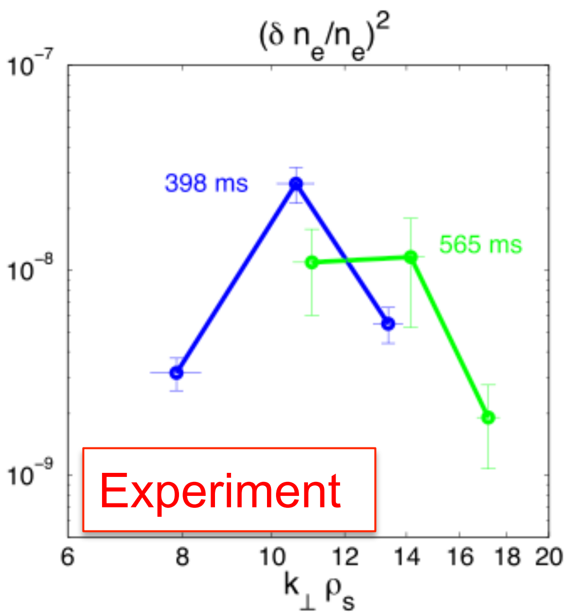

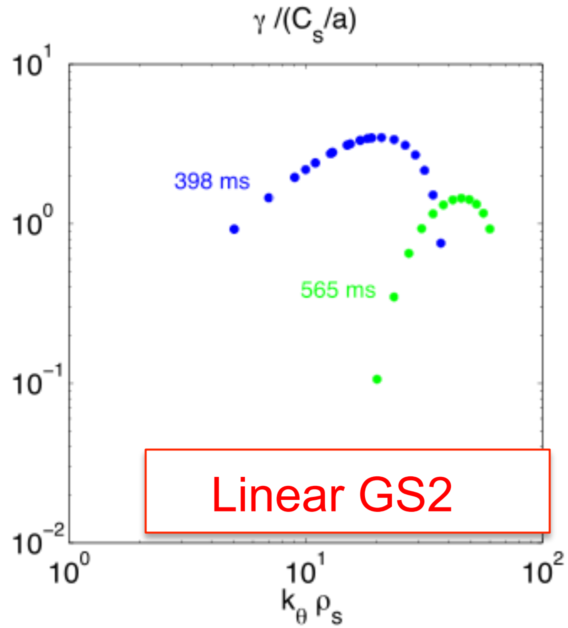

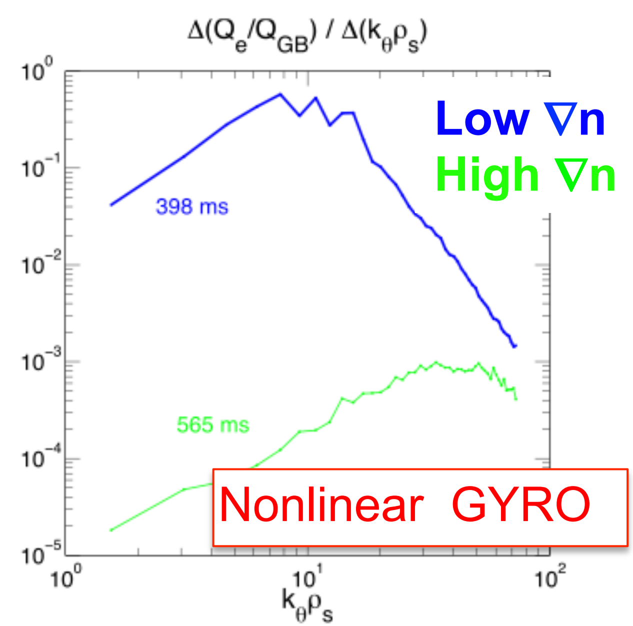

Electron Scale Turbulence Cannot Explain Experimental Electron Heat Flux

- Previous simulation work focused on electron scale turbulence.
- Low-k turbulence was assumed stabilized due to high ExB shear:
  - ω_{ExB} ~ low-k growth rate γ.
  - Neoclassical levels of Q_i.

- Electron heat flux from experiment & gyrokinetic simulation is reduced at high density gradient

	Low ∇n (t=398ms) $R/L_{ne} = 1.5$	High ∇n (t=565ms) $R/L_{ne} = 6.2$
$Q_e^{(exp)}$ [MW]	1.5	0.9
$Q_e^{(sim)}$ [MW]	0.4	$<10^{-2}$

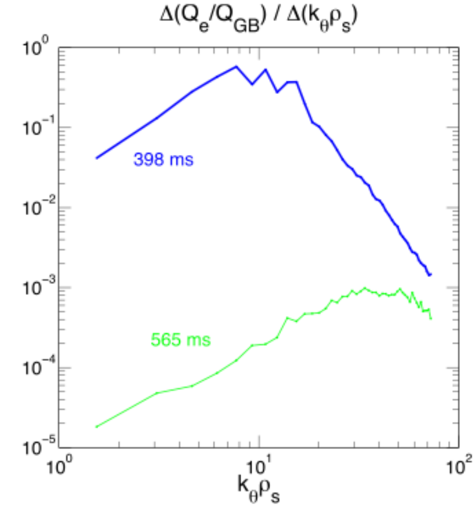

- For more details *cf.* Ruiz Ruiz PoP 2015.

- **Where is missing Q_e coming from?**

Probe Origins of Anomalous Electron Heat Flux Using Two Different Approaches:

1. Revisit the assumption:

***'Ion scale turbulence is suppressed by ExB shear in NSTX NBI heated H-mode plasmas'*.**

Approach: Identify ion scale instability and ion scale turbulence contributions to Q_e using linear and nonlinear gyrokinetic simulation (GYRO).

2. To what level of confidence do we trust transport predictions from previous e-scale simulations?

Approach: **Develop a synthetic high-k scattering diagnostic** for quantitative comparisons between electron scale turbulence measurements and nonlinear GYRO simulations.

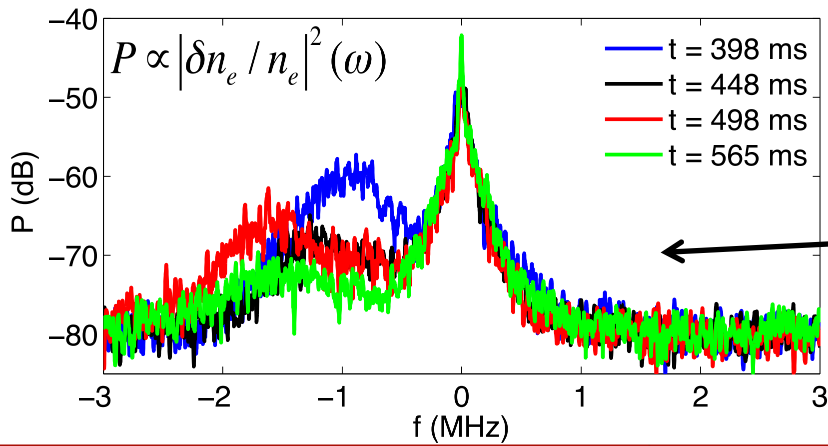

High-k scattering measurements

1. Revisit the assumption "*ion scale turbulence is suppressed by ExB shear*".

Outline

- Characterization of linear ion scale instability at low and high ∇**n** (slides 7).
- Electron thermal transport due to ion scale turbulence at low and ∇**n** (slides 8,9)**.**
- Summary of ion scale turbulence studies (slide 10).

Ion Scale Instability is Marginally Stable at **Low ∇n**, Driven Highly Unstable by Parallel Flow Shear at **High ∇n**

Low ∇n (blue)

- $\omega_{ExB} \geq \gamma$ → suggests ion scale turbulence is stabilized.
- Parallel flow shearing rate γ_p has little effect on growth rate (+ 20%).
- $A_{||}$ & $B_{||}$ fluctuations have little effect on γ_p (+ 20%).
- Ballooning mode structure.

High ∇n (green)

- $\gamma >> \omega_{ExB}$ → unstable ion scale turbulence!
- γ_p increases growth rate >100%, drives mode propagation in ion direction (-)
- $A_{||}$ & $B_{||}$ fluctuations have big effect on growth rate (+70%).
- Ballooning mode structure.
- Driven by ∇T_e, β, $B_{||}$, stabilized by ∇T_i, β', $A_{||}$.

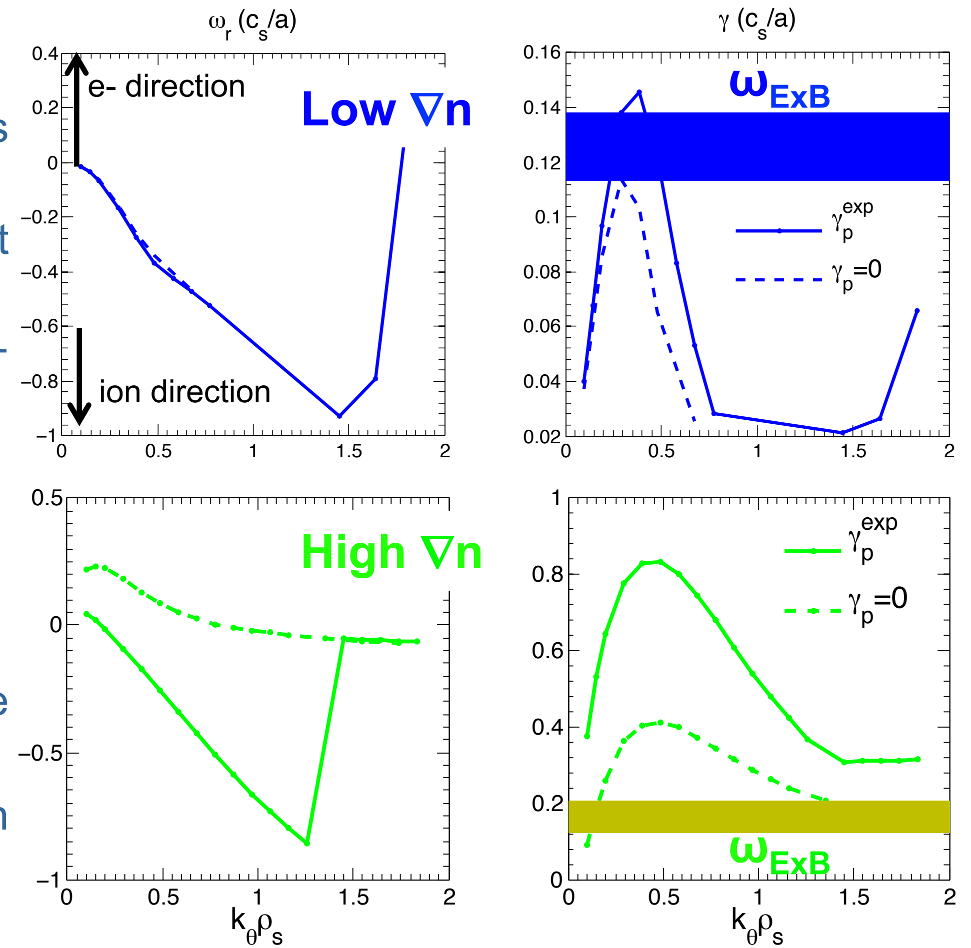

Parallel flow shearing rate (GYRO) γ_p, ω_0 toroidal rotation frequency

$$\gamma_p = -R_0 \frac{\partial \omega_0}{\partial r}$$

Local Ion Scale Nonlinear Gyrokinetic Simulation Shows Ion Scale Turbulence is Negligible at **Low ∇n**

- Negligible Q_e and Q_i from electrostatic (ES) & electromagnetic (EM) ion scale local gyrokinetic simulation at r/a~0.7 (GYRO).
  - Simulations included ExB + parallel flow shear.
- Electron scale simulation showed ~0.45MW (30% Q_e).
- Missing Q_e^{exp} remains unexplained.

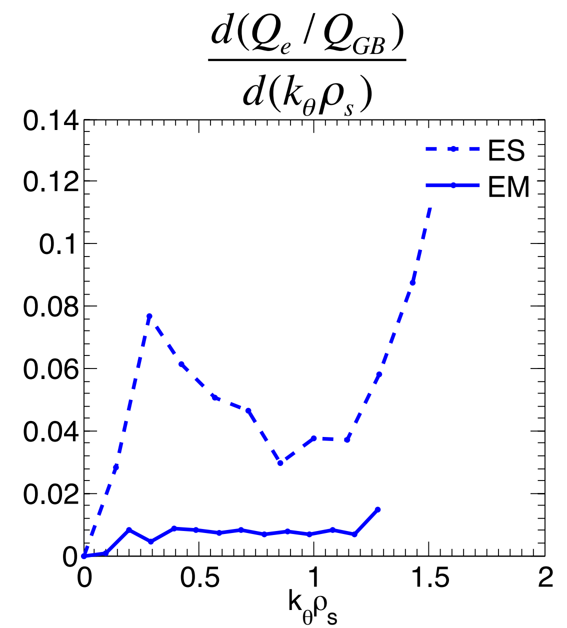

Low ∇n		
	Q_e	**Q_i**
Experiment (TRANSP)	1.5 MW	0.25 MW
ES ion scale GYRO (all gk)	10^{-2} MW	2.10^{-3} MW
	0.1 Q_{gB}	2.10^{-2} Q_{gB}
EM ion scale GYRO (all gk)	10^{-3} MW (all ES!)	$<10^{-4}$ MW
	10^{-2} Q_{gB}	~ 10^{-4} Q_{gB}

- *cf.* summary + backup slides for numerical resolution details.

Local Ion Scale Nonlinear Gyrokinetic Simulation Shows High ES Transport at **High ∇n**, Stabilized by EM effects

- High electron heat flux levels predicted by ES ion scale simulation (Fig. 1).
- Q_e is reduced a factor ~200 by including $\delta A_{||} + \delta B_{||}$ (Fig. 2).
  - Electromagnetic stabilization of ion scale turbulence.
  - Simulations included ExB + parallel flow shear.
- Electron scale simulation showed $Q_e < 10^{-2}$ MW.
- Q_e^{exp} remains unexplained.

High ∇n		
	Q_e	Q_i
Experiment (TRANSP)	1 MW	0.2 MW
ES ion scale GYRO (dke)	3.2 MW	1.3 MW
	23.6 Q_{gB}	9.3 Q_{gB}
EM ion scale GYRO (dke)	~2.10^{-3} MW	~2.10^{-3} MW
	~2.10^{-2} Q_{gB}	~2.10^{-2} Q_{gB}

- *cf.* summary + backup slides for simulation details.

$$\frac{d(Q_e/Q_{GB})}{d(k_\theta \rho_s)}$$

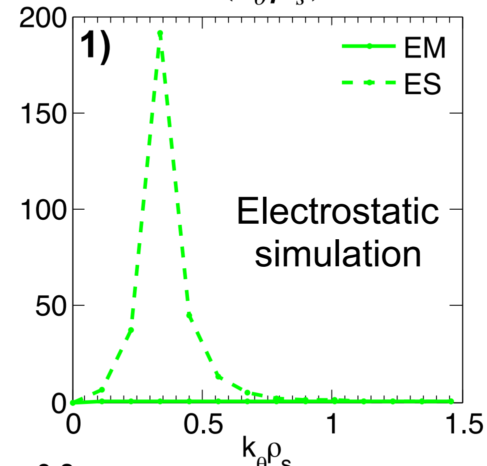

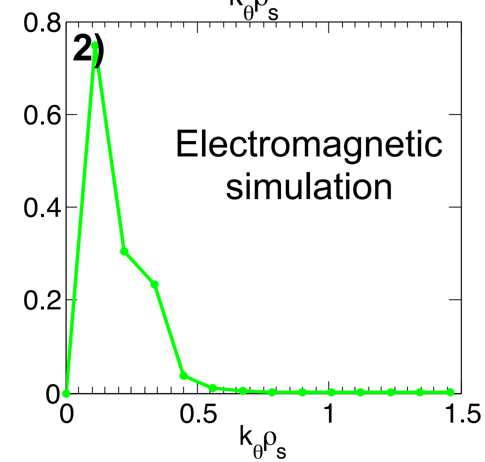

Ion Scale Simulations Presented Cannot Explain Q_e^{exp} neither at **Low** nor **High** ∇**n**

- Numerical Simulation details of local, ion scale simulations (r/a~0.7)
  - 3 gk species (e-, D, C), Z_{eff}~1.85-1.95
  - EM: $A_{||}+B_{||}$, β_e~ 0.3 %
  - collisions (ν_{ei} ~ 1 c_s/a)
  - ExB shear and parallel flow shear (γ_E~0.13-0.16 c_s/a, γ_p~1-1.2 c_s/a).

- Summary and future work on ion scale turbulence:

	Low ∇n	**High ∇n**
e- scale: Q_e^{sim}/Q_e^{exp}	~30%	<1%
ion scale: Q_e^{sim}/Q_e^{exp}	<0.1%	~0.2%

  - High ∇**n** case is disconcerting! **Q_e^{sim}(e- scale)+Q_e^{sim}(ion scale) < 1% Q_e^{exp}**
  - Further characterize unstable ion scale mode at **high ∇n** (linear GYRO).
  - Ion scale simulations presented are low resolution: need higher resolution runs
    - Linear GS2 suggests presence of unstable modes at $k_\theta\rho_s$ < 0.1 driven by β.
    - Q_e spectrum peaks at lowest resolved k ($k_\theta\rho_s$ ~ 0.1!) – *cf.* slide 9.
  - Study profile effects using global simulation (radial box L_r/a~0.3-0.5!).

Outline

- Operation of old high-k scattering diagnostic + Previous work on synthetic high-k scattering (slide 12).
- Preambles + Preliminary steps (slide 13).
- Implementation of Synthetic Diagnostic (slides 14-17)
  - Coordinate mapping:
    - Prerequisites (slide 15)
    - Jacobian Transformation (slide 16)
  - Filtering (ongoing work)
- Results from Coordinate Mapping (18-23).

Operation of Old High-k Microwave Scattering Diagnostic System at NSTX

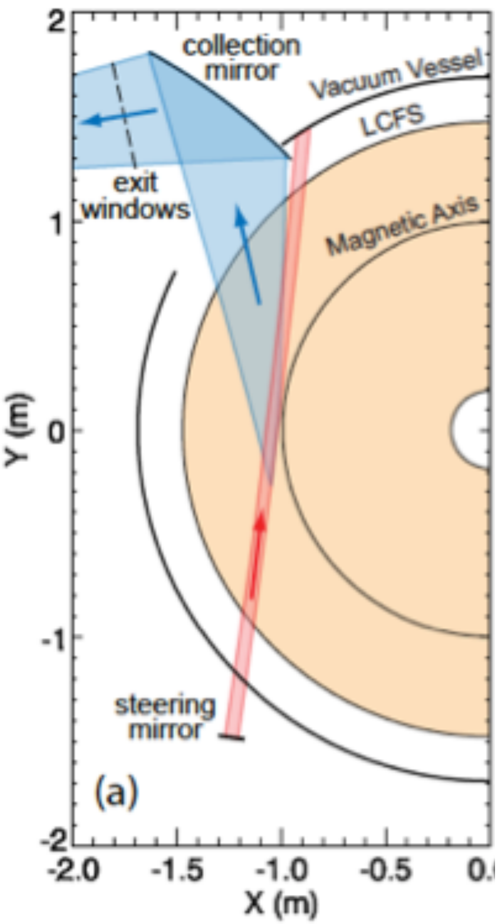

View from top of NSTX (D.R. Smith PhD thesis 2009)

Old High-k Scattering System

- Gaussian Probe beam: 15 mW, 280 GHz, λ_i ~ 1.07 mm, a = 3cm (1/e^2 radius).
- Propagation close to midplane => k_r spectrum.
- 5 detection channels => range k_r ~ 5-30 cm-1 (high-k).
- Wavenumber resolution $\Delta k = \pm 0.7$ cm-1.
- Radial coverage: R = 106-144 cm.
- Radial resolution: $\Delta R = \pm 2$ cm (unique feature).

Previous Work on Synthetic high-k

cf. Poli PoP 2010

- Previous synthetic high-k scattering was implemented with GTS (*cf.* Wang PoP 2006).
- Synthetic spectra affected by systematic errors (simulation run time, low k_θ detected)

Preliminary Steps Prior to the Implementation a Synthetic High-k Scattering Diagnostic using GYRO

Preambles:

- Scattering data from the high-k scattering system is spatially localized: scattering location is (R_{loc}, Z_{loc}, φ_{loc}) (cylindrical coordinates).
- Scattering data is sensitive to a particular turbulence wavenumber (k_R^{exp}, k_Z^{exp}).

Preliminary Steps:

- Obtain experimental high-k density fluctuation data → $|\delta n_e|^2_{kR,kZ}(\omega)$
- Use a ray tracing code to determine:
  - Scattering location + resolution→ (R_{loc}, Z_{loc}) + (ΔR_{loc}, ΔZ_{loc}).
  - Wavenumber response + resolution → (k_R^{exp}, k_Z^{exp}) + (Δk_R^{exp}, Δk_Z^{exp}).
- Run a nonlinear gyrokinetic simulation (used GYRO here) capturing scattering location + resolving experimentally measured wavenumber.

Summary Steps to Implementing a Synthetic High-k Scattering Diagnostic using GYRO

Steps in synthetic diagnostic implementation

- **Coordinate Mapping:**

  Coordinate mapping GYRO (r,θ,φ) ←→ physical (R, Z, φ)

  Wavenumber mapping $(k_r\rho_s, k_\theta\rho_s)_{GYRO}$ ←→ (k_R, k_Z)

  - Compute (r_{loc}, θ_{loc}) by nonlinear solve of $\{ R(r_{loc}, \theta_{loc}) = R_{loc}, Z(r_{loc}, \theta_{loc}) = Z_{loc}\}$.
  - Compute (k_r, k_θ)-grid (GYRO coordinates).
  - Compute $(k_r^{exp}, k_\theta^{exp})$ by mapping from (k_R^{exp}, k_Z^{exp}).

- **Filtering:** Apply instrumental selectivity function to simulated density fluctuations

  - Define selectivity function on local grid (k_r,k_θ)-grid (*cf.* Mazzucato PoP 2003, PPCF 2006).
  - Interpolate δn_e to obtain fluctuation spectrum in (k_θ, k_r)-grid.
  - Apply (k_r,k_θ) filtering to δn_e → synthetic signal $\delta n_e(t)$ → $\delta n_e^{syn}(\omega)$.

In this poster, will only focus on **Mapping**. Filtering is part of ongoing work.

Prerequisites to Coordinate Mapping

<u>We want to perform:</u>

- *coordinate mapping GYRO (r,θ,φ) ←→ physical (R, Z, φ)*
- *wavenumber mapping $(k_r\rho_s, k_\theta\rho_s)_{GYRO}$ ←→ (k_R, k_Z)*

<u>Prerequisites</u>

- Units: r[m], R[m], Z[m], $\theta, \varphi \in [0,2\pi]$
- **GYRO definition of** k_θ^{loc} and k_θ^{FS}

$$k_\theta^{loc}(r,\theta) = -\frac{n}{r}\frac{\partial \nu}{\partial \theta}, \quad k_\theta^{FS} = \frac{nq}{r}$$

Consistent with GYRO definition of flux-surface averaged $k_\theta^{FS}=nq/r$ (*cf.* backup)

- Wavenumber mapping under simplifying assumptions

$$\boxed{k_R = (k_r\rho_s)_{GYRO}\left|\nabla r\right| / (\rho_s)_{GYRO}}$$

$$\boxed{k_Z = (k_\theta\rho_s)_{GYRO}^{loc} / (\kappa.\rho_s)_{GYRO}}$$

- Miller-like parametrization
- $\zeta=0$, $d\zeta/dr=0$ (squareness)
- $Z_0=0$, $dZ_0/dr=0$ (elevation)
- UD symmetric (up-down symmetry)
  →$(\theta=0)$

Mapping $(R, Z, \varphi) \rightarrow (r, \theta, \varphi)$
$(k_R, k_Z) \rightarrow (k_r, k_\theta)$

Jacobian transformation + definitions of k_R, k_Z, k_r, k_θ

$$\begin{pmatrix} \dfrac{\partial}{\partial r} \\ \dfrac{\partial}{\partial \theta} \end{pmatrix} = \begin{pmatrix} \dfrac{\partial R}{\partial r} & \dfrac{\partial Z}{\partial r} \\ \dfrac{\partial R}{\partial \theta} & \dfrac{\partial Z}{\partial \theta} \end{pmatrix} \begin{pmatrix} \dfrac{\partial}{\partial R} \\ \dfrac{\partial}{\partial Z} \end{pmatrix} \quad + \quad \begin{cases} ik_R = \dfrac{\partial}{\partial R}, \quad ik_Z = \dfrac{\partial}{\partial Z} \\ ik_r = \dfrac{\partial}{\partial r}, \quad ik_\theta^{loc} = \dfrac{1}{r}\dfrac{\partial}{\partial \theta} \end{cases}$$

$$\Rightarrow \boxed{\begin{cases} k_r = k_R \dfrac{\partial R}{\partial r} + k_Z \dfrac{\partial Z}{\partial r} \\ k_\theta^{loc} = k_R \dfrac{1}{r}\dfrac{\partial R}{\partial \theta} + k_Z \dfrac{1}{r}\dfrac{\partial Z}{\partial \theta} \end{cases}}$$

- **Need to compute ∂R/∂r, ∂R/∂θ, ∂Z/∂r, ∂Z/∂θ @ (r_{loc}, θ_{loc})**
- Will obtain $(k_r,k_\theta)_{exp}$ in GYRO coordinates!

Complete GYRO-Real Space Wavenumber Mapping

The complete wavenumber mapping is

$$\boxed{k_r = k_R \frac{\partial R}{\partial r} + k_Z \frac{\partial Z}{\partial r}}$$

$$\boxed{k_\theta^{loc} = k_R \frac{1}{r}\frac{\partial R}{\partial \theta} + k_Z \frac{1}{r}\frac{\partial Z}{\partial \theta}}$$

- Derivatives are computed at (r_{loc}, θ_{loc}), and $k_R = k_R^{exp}$, $k_Z = k_Z^{exp}$ (determined by ray-tracing calculations).
- This mapping reduces to simplified mapping in slide 15 for θ=0+UD sym.
- Computed GYRO Geometric Coefficients (∂R/∂r, …) agree with GYRO output.

Calculated $(k_r,k_\theta)^{exp}$ in GYRO Geometry

Given from experiment (ray tracing)

k_R = -1857 m^{-1}, k_Z=493 m^{-1} (channel 1 of high-k diagnostic)

Get from GYRO (internally calculated)

- $(\rho_s)_{GYRO}$ ~ 0.002 m (B_unit ~ 1.44)
- $|\nabla r|$ ~ 1.43, κ ~ 2

Apply mapping (simplified approx.)

$$\begin{cases} (k_r\rho_s)_{GYRO} = k_R * (\rho_s)_{GYRO} / |\nabla r| \\ (k_\theta\rho_s)^{loc}_{GYRO} = k_Z * \kappa * (\rho_s)_{GYRO} \end{cases}$$

cf. slide 15

Obtain experimental wavenumbers mapped to GYRO

$(k_r\rho_s)_{GYRO}$~ -2.6

$(k_\theta\rho_s)_{GYRO}$~ 2.0

Mapped $(k_R, k_Z)^{exp}$ to GYRO $(k_r\rho_s, k_\theta\rho_s)_{GYRO}$

(k_r, k_θ) mapping in a high-resolution, e- scale GYRO simulation of real NSTX plasma discharge (141767).

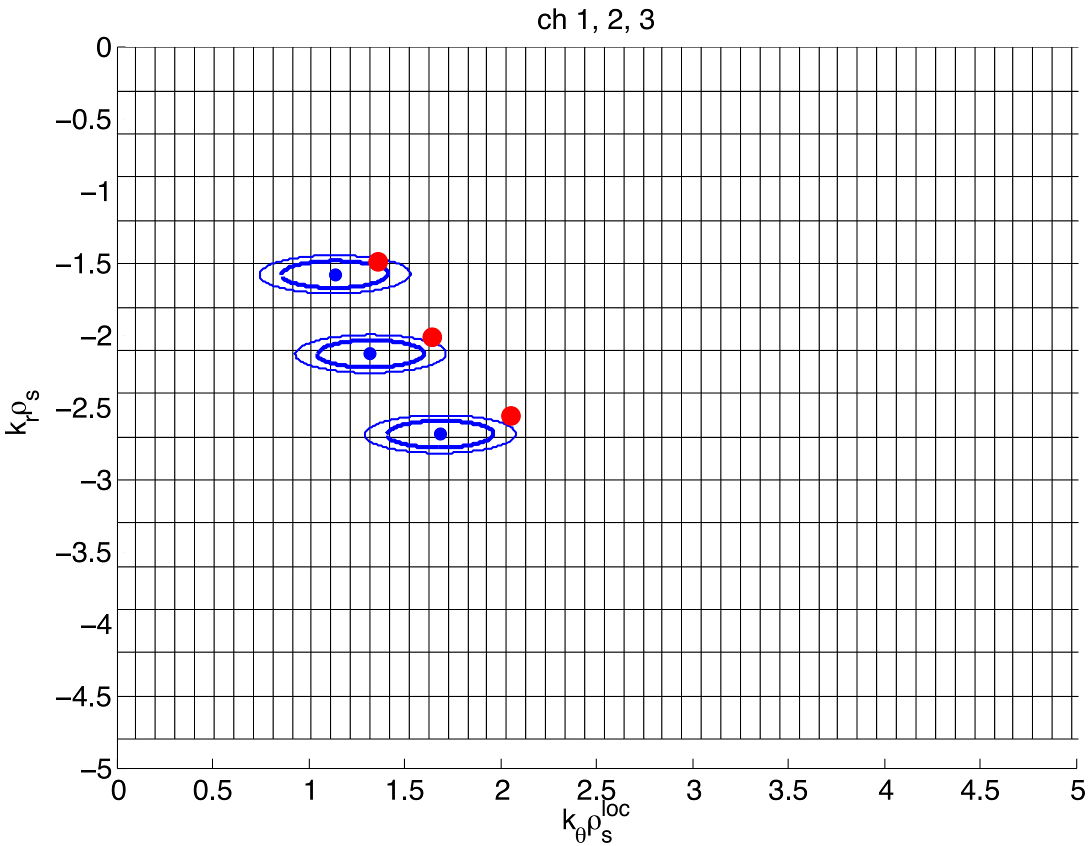

- **Red dots:** (k_r, k_θ) assume θ_{loc}=0 approx (*cf.* slide 15,18).

$$\begin{cases} (k_r\rho_s)_{GYRO} = k_R * (\rho_s)_{GYRO} / |\nabla r| \\ (k_\theta\rho_s)^{loc}_{GYRO} = k_Z * \kappa * (\rho_s)_{GYRO} \end{cases}$$

- **Blue dots:** (k_r, k_θ) $\theta=\theta_{loc}$ (~-0.06 rad) (complete mapping)
- Ellipses are e^{-1} and e^{-2} amplitude of (k_r, k_θ) gaussian filter (simplified selectivity function)

$$F(k_r, k_\theta) = F_r(k_r)F_\theta(k_r)$$

$$F_r(k_r) = \exp\left(-(k_r - k_r^{\exp})^2 / \Delta k_r^2\right)$$

$$F_\theta(k_\theta) = \exp\left(-(k_\theta - k_\theta^{\exp})^2 / \Delta k_\theta^2\right)$$

Resolving $(k_R,k_Z)^{exp}$ + Complete ETG Spectrum Requires a Big-Simulation-Domain e- Scale Simulation

Resolution constrains:

- Resolve $(k_R,k_Z)^{exp}$ → $\Delta k_\theta \rho_s^{FS} \sim 0.3$.
- Resolve full ETG spectrum → $(k_\theta \rho_s^{FS})^{max} \sim 43$.
- Radial overlap with scattering beam width → $L_r \sim 8$ cm ($L_r \sim 21\ \rho_s$)
- Resolve e- scale turbulence eddies → $\Delta r \sim 2\rho_e$.

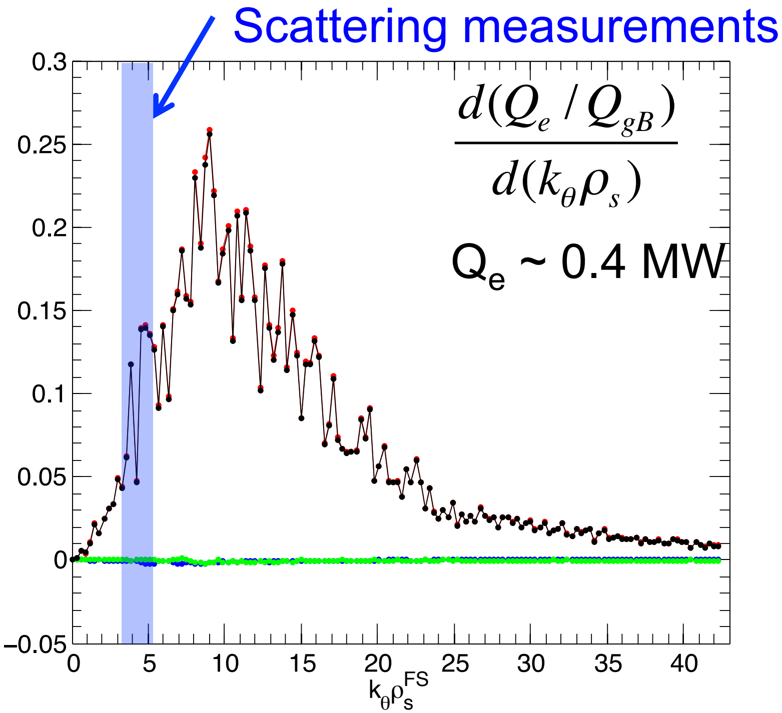

Resolution parameters

	Standard e-scale	Big-box e-scale
$L_r\ [\rho_s]$	6	21
$L_y\ [\rho_s]$	6	21
$\Delta r\ [\rho_e]$	~ 2	2.5
n_r (radial grid)	~ 200	512
$\Delta k_\theta \rho_s$	1-1.5	0.3
$k_\theta \rho_s^{max}$	40-50	43
n (tor. modes)	~50	142

$k_\theta \rho_s$ here means $k_\theta \rho_s^{FS}$

- Spectra show well resolved $(k_R,k_Z)^{exp}$ and ETG spectrum (*cf.* slide 22).
- Experimental wavenumbers produce non-negligible δn_e and Q_e consistent with previous e- scale simulation results ($Q_e \sim 0.4$ MW).

A Big-Simulation-Domain Electron Scale Simulation Was Performed to Apply New Synthetic Diagnostic

- Outboard mid-plane $\delta n_e(R, Z)$ in high resolution e- scale GYRO simulation of real NSTX plasma discharge.
- Shot 141767, time t = 398 ms (*cf.* Ruiz Ruiz PoP 2015).
- Scattering location and scattering volume extent are within GYRO simulation domain.
- Dots are scattering location for channels 1, 2, and 3 of high-k diagnostic.
- Dashed circles are 3cm and √2*3 cm microwave beam radii (for channel 1).

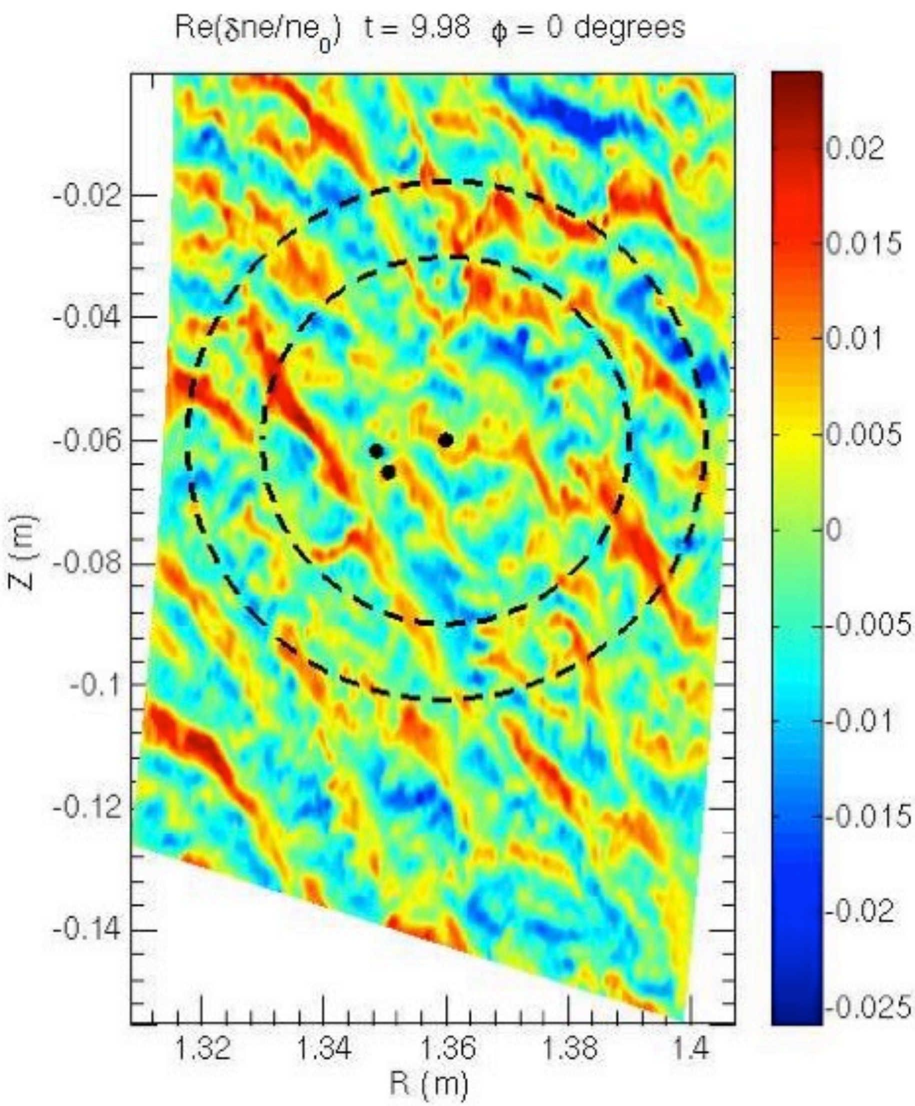

Mapped Experimental Wavenumbers in GYRO Density Spectra

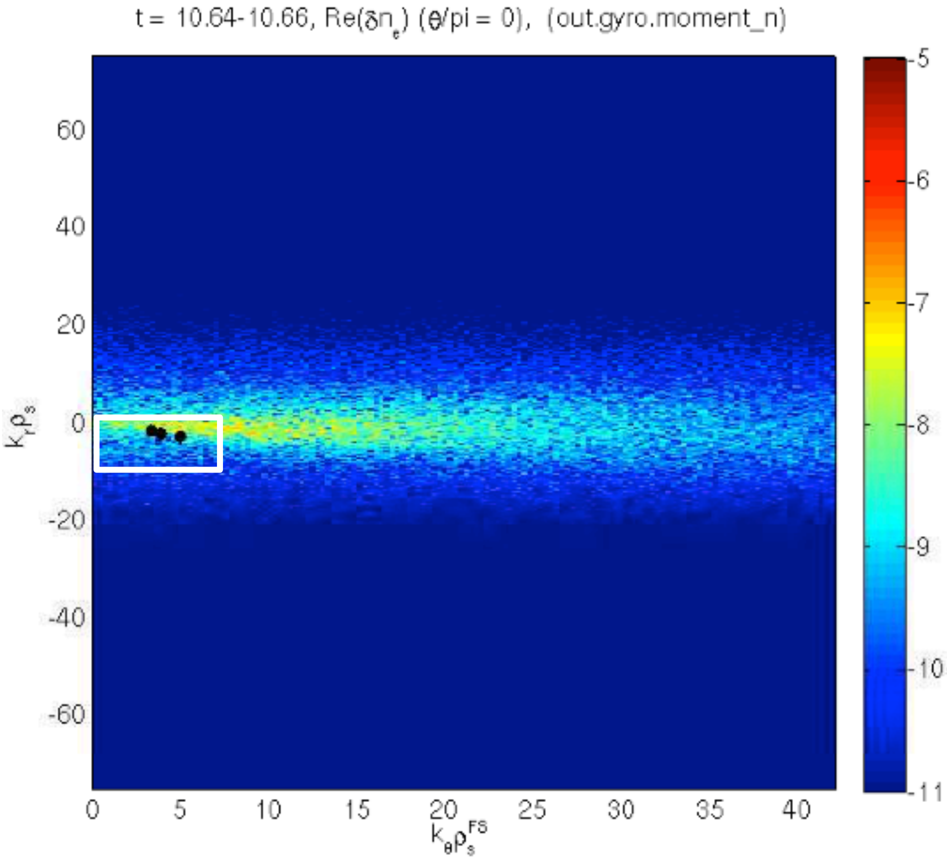

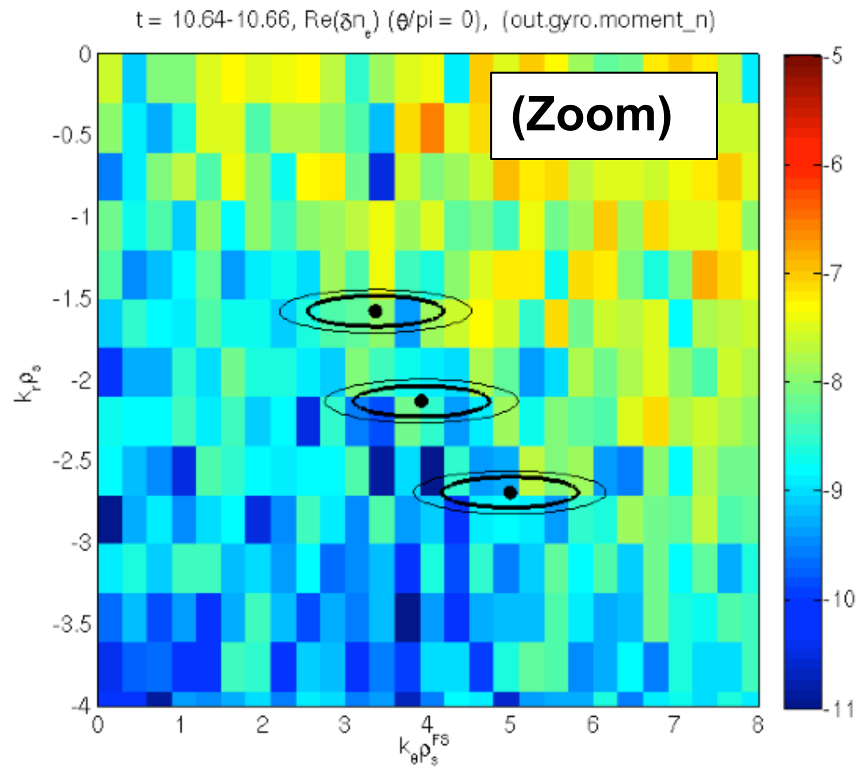

$$k_\theta^{FS} = \frac{1}{2\pi}\int_0^{2\pi} k_\theta^{loc}\, d\theta = \frac{nq}{r}$$

- **Note**: Plotting $k_\theta \rho_s^{FS}$, not $k_\theta \rho_s^{loc}$!!
- **Black dots:** scattering $(k_r, k_\theta)^{exp}$ for channels 1,2,3 (note in these figures, spectrum is output at θ=0, and black dots correspond to θ~-0.06 rad).
- **Ellipses:** e^{-1} and e^{-2} amplitude of (k_r, k_θ) gaussian filter (simplified selectivity function).

Numerical Resolution Details of Ion and Electron Scale Simulations Presented

Experimental profiles used as input

Local, flux tube simulations performed at scattering location (r/a~0.7, R~136 cm).

- Only electron scale turbulence included.
- Experimental T_e, n_e, T_i, rotation, etc.
- 3 kinetic species, D, C, e (Z_{eff}~1.85-1.95)
- Electromagnetic: $A_{||}+B_{||}$, β_e~ 0.3 %.
- Collisions (ν_{ei} ~ 1 c_s/a).
- ExB shear (γ_E~0.13-0.16 c_s/a) + parallel flow shear (γ_p ~ 1-1.2 c_s/a)
- Fixed boundary conditions with Δ^b ~ 8/1.5 ρ_s buffer widths (ion/e- scale).

Ion scale resolution parameters

- $L_r \times L_y = 74 \times 56\ \rho_s$ (L/a~0.4).
- $n_r \times n = 192 \times 14$.
- $k_\theta \rho_s^{FS}$ [min, max] = [0.1, 1.4]
- $k_r \rho_s$ [min, max] =[0.85, 4]
- $[n_{||}, n_\lambda, n_e]$ = [14, 12, 12]

Big-box e- scale resolution parameters

- $L_r \times L_y = 21 \times 21\ \rho_s$ (L/a~0.16).
- $n_r \times n = 512 \times 142$.
- $k_\theta \rho_s^{FS}$ [min, max] = [0.3, 43]
- $k_r \rho_s$ [min, max] = [0.3, 38]
- $[n_{||}, n_\lambda, n_e]$ = [14, 12, 12]

High-resolution electron scale runs presented here are NOT multiscale:

- Ions are not resolved correctly $\Delta k_\theta \rho_s$~0.3, $L_r \times L_y = 21 \times 21\ \rho_s$.
- Simulation ran only for electron time scales (~20a/c_s), ions are not fully developed.

Summary and Future Work on Synthetic Diagnostic Implementation

Summary

- Completed coordinate transformation and wavenumber mapping from GYRO space to real space.
- A big-box electron scale simulation is needed to simultaneously resolve full ETG spectrum and experimental wavenumbers in old high-k system.
- Experimental wavenumbers produce non-negligible δn_e and Q_e, consistent with previous e- scale simulation predictions.

Future work

- Implementation of selectivity function and filtering → quantitative comparisons with experiment!
- Project operating space of new high-k diagnostic.
- Study turbulence characteristics in high-resolution e- scale run → towards multiscale simulation in NSTX-U.

This work is supported by US. D.O.E. Contract No. DE-AC02-09CH11466. Computer simulations were carried out at the National Energy Research Scientific Computing Center, US. D.O.E. Contract No. DE-AC02-05CH11231.

Back-up slides

Numerical Resolution Comparison with Traditional Ion Scale, Electron Scale and Multiscale Simulation

Poloidal wavenumber resolution ($k_\theta \rho_s$ here means $k_\theta \rho_s^{FS}$)

	$\Delta k_\theta \rho_s$	$k_\theta \rho_s^{max}$	n #tor. modes
Ion scale	~0.05	~1	~20-30
e- scale	~1-1.5	~50	~50
Multi-scale	~0.1	~40	~500
High res. e- scale	**0.3**	**43**	**142**

Radial resolution Δr– radial box size L_r

	Δr	L_r	n_r radial grid
Ion scale	~ 0.5 ρ_s	~80-100 ρ_s	~ 200
e- scale	~ 2 ρ_e	~ 6-8 ρ_s	~ 200
Multi-scale	~ 2 ρ_e	~ 40-60 ρ_s	~ 1500
High res. e- scale	**2.5 ρ_e**	**20 ρ_s**	**512**

Input Parameters into Nonlinear Gyrokinetic Simulations Presented

	t=398	t = 565
r/a	0.71	0.68
a [m]	0.6012	0.596
n_e [10^19 m-3]	4.27	3.43
T_e[keV]	0.39	0.401
a/L_{ne}	1.005	4.06
a/L_{Te}	3.36	4.51
β_e^{unit}	0.0027	0.003
a/L_{nD}	1.497	4.08
a/L_{Ti}	2.96	3.09
T_i/T_e	1.13	1.39
n_D/n_e	0.785030	0.80371
n_c/n_e	0.035828	0.032715
a/L_{nC}	-0.87	4.08
a/L_{TC}	2.96	3.09
Z_{eff}	1.95	1.84
nu_{ei} (a/c_s)	1.38	1.03
q	3.79	3.07
s	1.8	2.346

R_0/a	1.52	1.59
SHIFT $=dR_0/dr$	-0.3	-0.355
KAPPA = κ	2.11	1.979
s_k=rdln(κ)/dr	0.15	0.19
DELTA = δ	0.25	168
s_δ=rd(δ)/dr	0.32	0.32
M	0.2965	0.407
γ_E	0.126	0.1646
γ_p	1.036	1.1558
ρ_*	0.003	0.0035
λ_D/a	0.000037	0.0000426
c_s/a (10^5 s-1)	4.4	2.35
Qe (gB)	3.82	0.0436
Qi (gB)	0.018	0.0003

Mapping $(k_r\rho_s, k_\theta\rho_s)_{GYRO} \rightarrow (k_R, k_Z)^{exp}$

We want to perform:

- *coordinate mapping GYRO (r,θ,φ) $\leftrightarrow$ physical (R, Z, φ)*
- *wavenumber mapping $(k_r\rho_s, k_\theta\rho_s)_{GYRO}$ $\leftrightarrow$ (k_R, k_Z)*

Preamble 1

- Units: r[m], R[m], Z[m] $\theta, \varphi \in [0,2\pi]$
- **GYRO definition of** k_θ^{loc} and k_θ^{FS}

$$ik_\theta^{loc}(r,\theta) = \frac{1}{r}\frac{\partial}{\partial\theta} \Rightarrow k_\theta^{loc}(r,\theta) = -\frac{n}{r}\frac{\partial\nu}{\partial\theta}$$

(To be shown in slide 17)

Consistent with GYRO definition of flux-surface averaged $k_\theta^{FS}=nq/r$ (*cf.* out.gyro.run)

$$k_\theta^{FS} = \frac{1}{2\pi}\int_0^{2\pi} k_\theta^{loc}\, d\theta = \frac{1}{2\pi}\int_0^{2\pi} -\frac{n}{r}\frac{\partial\nu}{\partial\theta} d\theta = \left(-\frac{n}{r}\right)\frac{\nu(r,2\pi)-\nu(r,0)}{2\pi} = \frac{nq(r)}{r}$$

Mapping $(k_r\rho_s, k_\theta\rho_s)_{GYRO} \rightarrow (k_R, k_Z)^{exp}$

<u>Preamble 2</u> why is $k_\theta^{loc}(r,\theta) = -\frac{n}{r}\frac{\partial \nu}{\partial \theta}$ **??**

GYRO decomposition of fields

$$\delta\phi(r,\theta,\alpha) = \sum_{j=-Nn+1}^{Nn-1} \delta\hat{\phi}_n(r,\theta)\mathrm{e}^{-in\alpha}\, e^{in\bar{\omega}_0 t} = \sum_{j=-Nn+1}^{Nn-1} \delta\phi_n(r,\theta), \quad \alpha = \varphi + \nu(r,\theta)$$

Set φ=0 and ω_0 = 0. Focus on transformation of one toroidal mode n. By definition of k_θ^{loc}

$$ik_\theta^{loc}\delta\phi_n(r,\theta) = \frac{1}{r}\frac{\partial}{\partial\theta}(\delta\phi_n(r,\theta)) = \frac{1}{r}\frac{\partial}{\partial\theta}(\delta\hat{\phi}_n(r,\theta)e^{-in\nu(r,\theta)}) =$$

$$\frac{1}{r}\left(\frac{\partial\delta\hat{\phi}_n}{\partial\theta}e^{-in\nu} + \delta\hat{\phi}_n\left(-in\frac{\partial\nu}{\partial\theta}\right)e^{-in\nu}\right) \Rightarrow \delta\phi_n(r,\theta)\left(\frac{-in}{r}\frac{\partial\nu}{\partial\theta}\right)$$

Conclusion: we assume definition of k_θ^{loc} is **correct.**
There is a one-to-one relation between n and k_θ^{loc} .

$$\boxed{k_\theta^{loc}(r,\theta) = -\frac{n}{r}\frac{\partial\nu}{\partial\theta}}$$

Mapping $(k_r\rho_s, k_\theta\rho_s)_{GYRO} \rightarrow (k_R, k_Z)^{exp}$

Preamble 3 Wavenumber mapping under simplifying assumptions

$$\boxed{k_R = (k_r\rho_s)_{GYRO}\left|\nabla r\right| / (\rho_s)_{GYRO}}$$

$$\boxed{k_Z = (k_\theta\rho_s)^{loc}_{GYRO} / (\kappa.\rho_s)_{GYRO}}$$

- Assumptions
  - $\zeta=0$, $d\zeta/dr=0$ (squareness + radial derivative)
  - $Z_0=0$, $dZ_0/dr=0$ (elevation + radial derivative)
  - UD symmetric (up-down asymmetry of flux surface)

- In the following slides, develop mapping when assumptions are not satisfied, invert

  $(R(r,\theta),Z(r,\theta))=(R_{exp}, Z_{exp}) \rightarrow (r_{exp},\theta_{exp})$.

Principle of Geometric Mapping is Independent of Flux Surface Parametrization

Computation of metric coefficients

- Whether you use a Model Grad-Shafranov equilibrium (GS, Miller-type) or a general equilibrium (Fourier), procedure is the same.

- In cases shown here, I use GS equilibrium.
  - In GYRO simulation, I use input parameters THETA_PLOT=8, THETA_MULT=128 (fine poloidal grid).
  - Get r[m] from out.gyro.profiles (use a_{ref} !!)
  - Create a θ array ∈[0,2π], size THETA_PLOT*THETA_MULT+1=1025.
  - Define R(r,θ) and Z(r, θ) (GS or general eq.). Used GS equilibrium here:

$$\begin{cases} R(r,\theta) = R_0(r) + r * \cos(\theta + \arcsin(\delta(r))\sin(\theta)) \quad [m] \\ Z(r,\theta) = Z_0(r) + r * \kappa(r) * \sin(\theta + \zeta(r)\sin(2\theta)) \quad [m] \end{cases}$$

- How am I sure that these derivatives are computed correctly?
  ➔Comparisons with output from out.gyro.geometry_arrays!

Computed GYRO Geometric Coefficients agree with GYRO output

$$|\nabla r|(r,\theta) = \frac{\left(\left(\frac{\partial R}{\partial \theta}\right)^2 + \left(\frac{\partial Z}{\partial \theta}\right)^2\right)^{1/2}}{\frac{\partial R}{\partial r}\frac{\partial Z}{\partial \theta} - \frac{\partial R}{\partial \theta}\frac{\partial Z}{\partial r}}$$

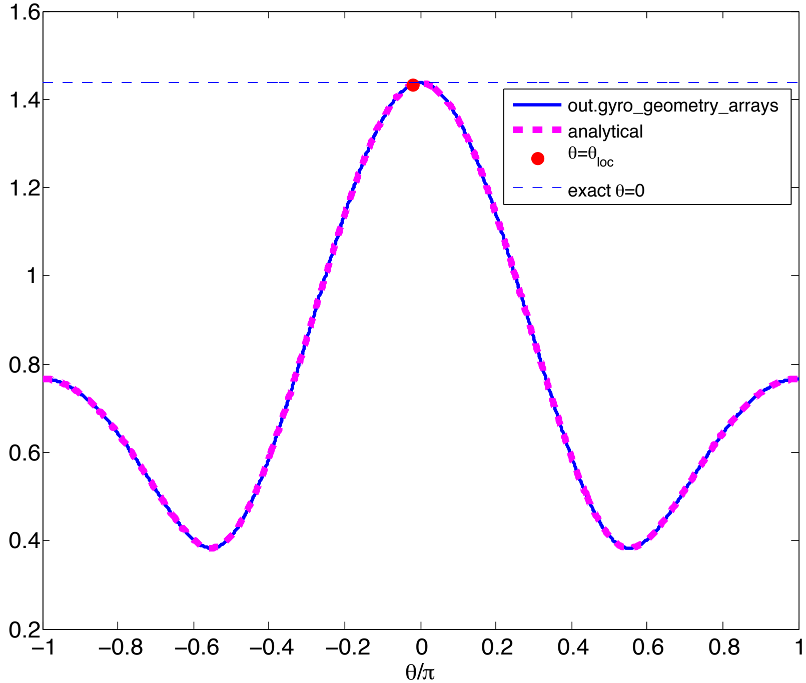

$$\sin u(r,\theta) = \frac{-\frac{\partial R}{\partial \theta}}{\left(\left(\frac{\partial R}{\partial \theta}\right)^2 + \left(\frac{\partial Z}{\partial \theta}\right)^2\right)^{1/2}}$$

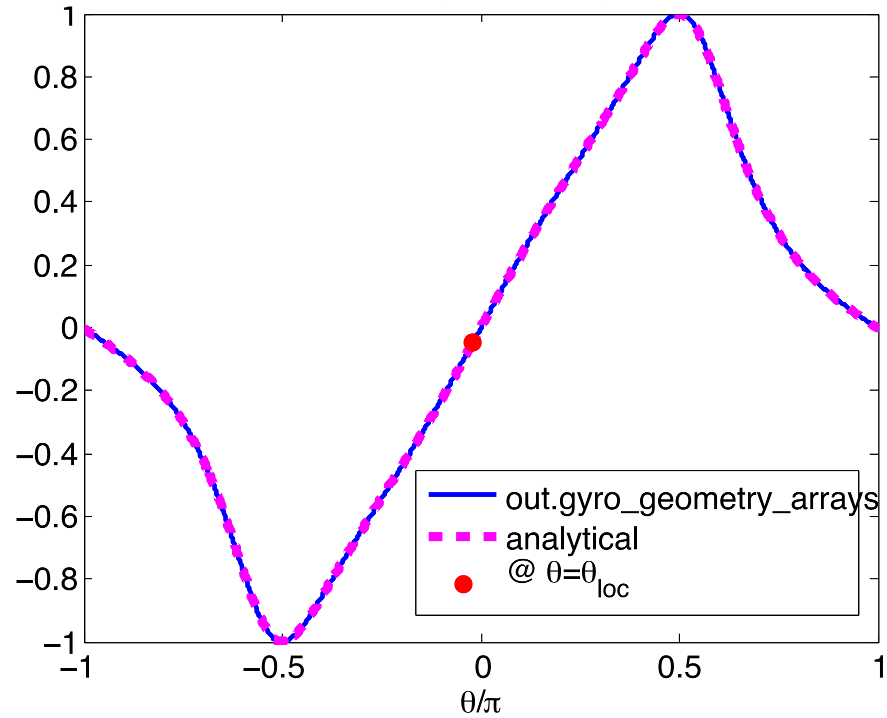

Conclusion: Agreement between output from out.gyro.geometry_arrays and computed coefficients gives us confidence the mapping is being performed correctly.

Poloidal Cross Section of High-Resolution Electron Scale Simulation

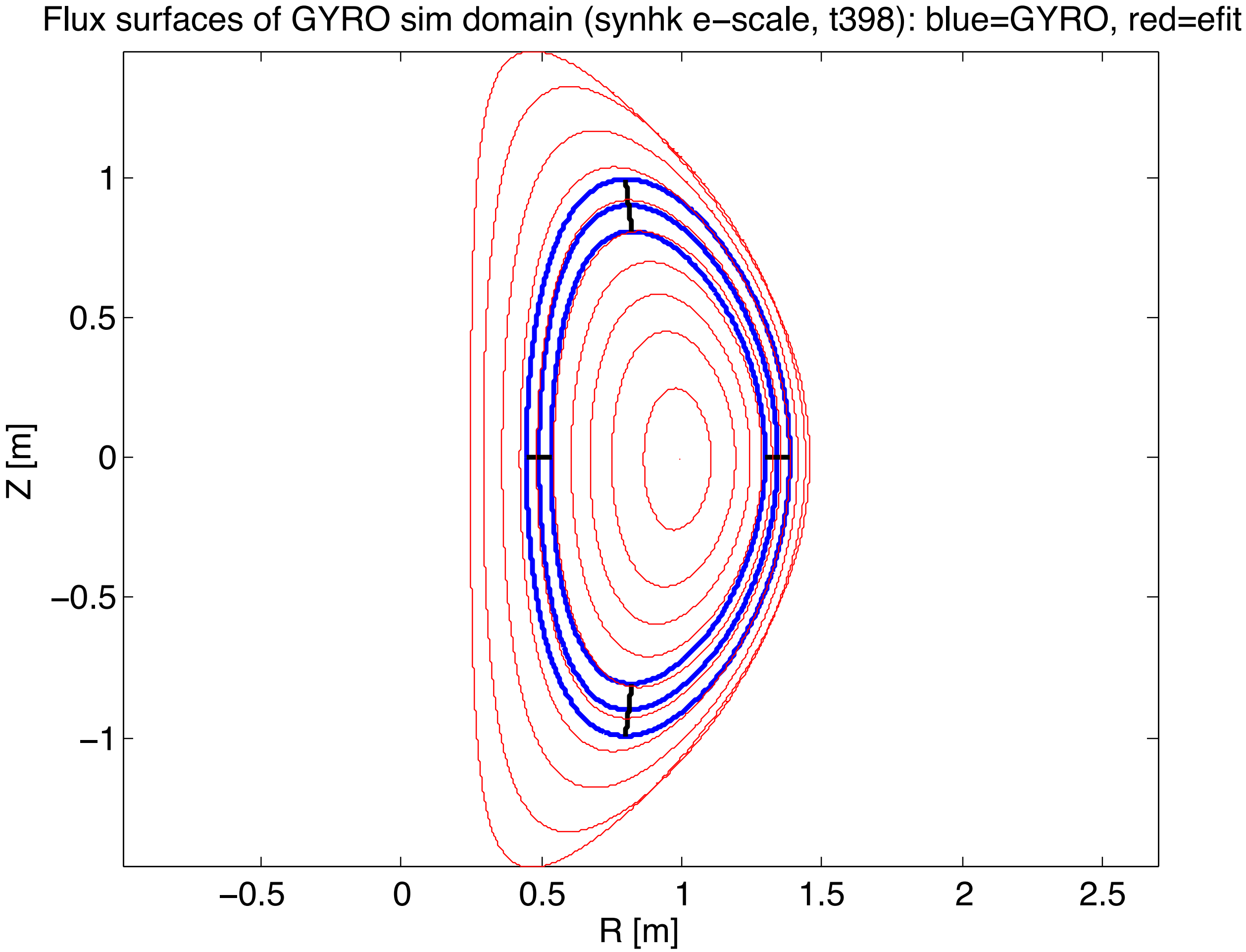

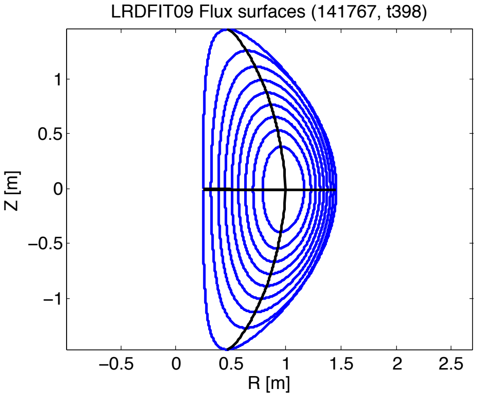

Local simulation
r/a ~ 0.7

Linear Growth Rates for Low-k and High-k Turbulence

- Note ion propagating high-k mode + electron propagating, non-balloning mode at krho~12.
- Microtearing turbulence?

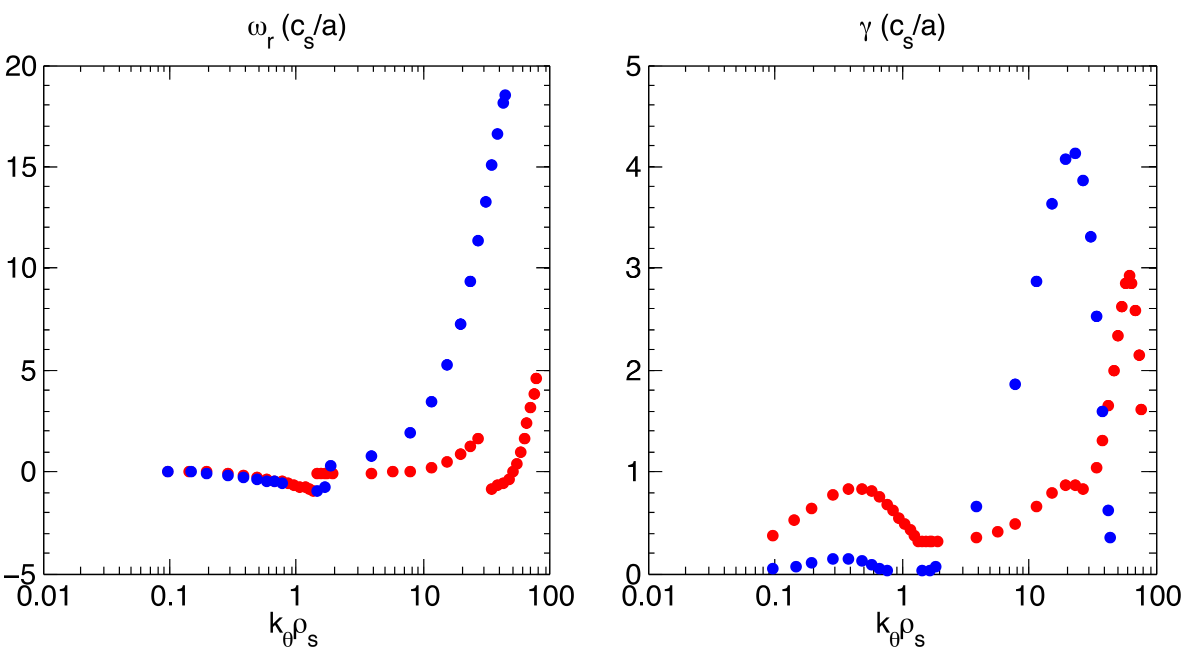

k_θ resolution in synhk GYRO sim.

<u>Huge e- scale run for syn hk</u> (tested it in debug! → 1h30m for 1 a/cs)

16,488 cores, ~ 24h, 4 open MP threads(4x4,032cores), Edison (x1.2) →**500,000 h (400,000h)**

Run for 20 a/cs

Distribution points 495,452,160

$$k_\theta^{loc} = -\frac{n}{r}\frac{\partial \nu}{\partial \theta}(\bar{r}, \theta = 0)$$

Radial and poloidal variation of $(k_\theta \rho_s)^{loc}$ [θ=0]

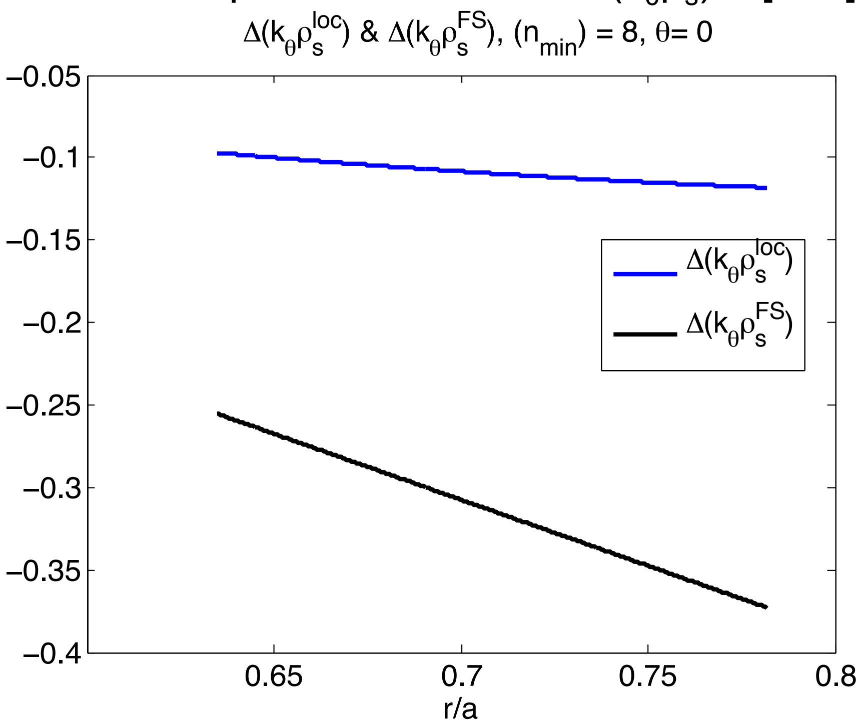

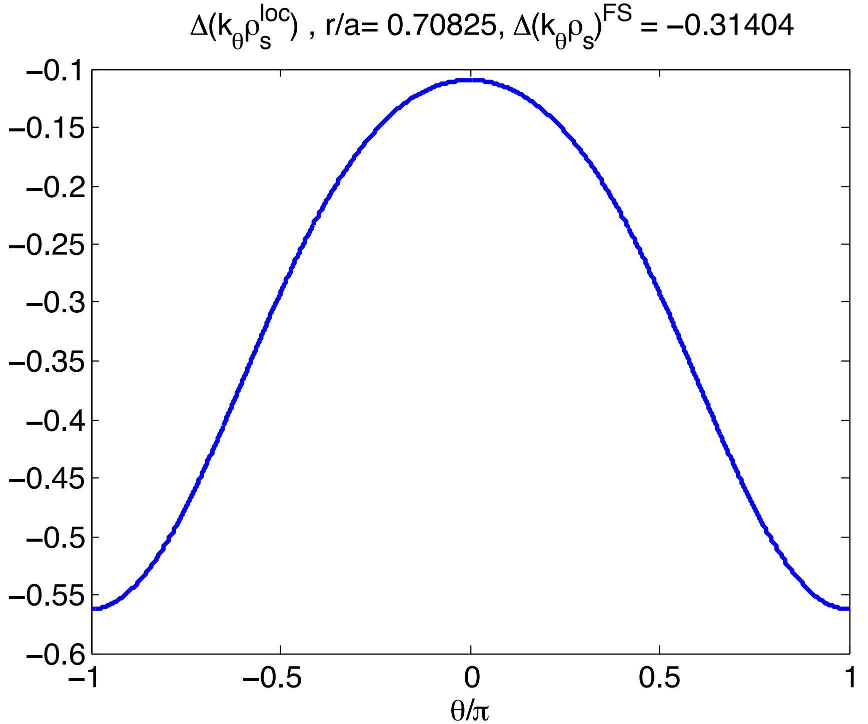

Appendix: Compute (Δk_R, Δk_Z) ➔($\Delta k_r \rho_s$, $\Delta k_\theta \rho_s$)^{GYRO}

Assume $\Delta k_R = \Delta k_Z = \Delta k = 66.7 m^{-1}$

$$\begin{cases} k_r = k_R \dfrac{\partial R}{\partial r} + k_Z \dfrac{\partial Z}{\partial r} \\ r k_\theta = k_R \dfrac{\partial R}{\partial \theta} + k_Z \dfrac{\partial Z}{\partial \theta} \end{cases} \Rightarrow \begin{cases} (\Delta k_r)^2 = (\Delta k_R)^2 \left(\dfrac{\partial R}{\partial r}\right)^2 + (\Delta k_Z)^2 \left(\dfrac{\partial Z}{\partial r}\right)^2 \\ (\Delta k_\theta)^2 = (\Delta k_R)^2 \left(\dfrac{1}{r}\dfrac{\partial R}{\partial \theta}\right)^2 + (\Delta k_Z)^2 \left(\dfrac{1}{r}\dfrac{\partial Z}{\partial \theta}\right)^2 \end{cases}$$

This assumes beam radius a = 3cm, such that $\Delta k = 2/a = 66.7 m^{-1}$
As a first approximation, assume simplest selectivity function: gaussian is k_r and k_θ

$$F(k_r, k_\theta) = F_r(k_r) F_\theta(k_r)$$

$$F_r(k_r) = \exp\left(-(k_r - k_r^{\exp})^2 / \Delta k_r^2\right)$$

$$F_\theta(k_\theta) = \exp\left(-(k_\theta - k_\theta^{\exp})^2 / \Delta k_\theta^2\right)$$

Inverse Mapping $(k_R, k_Z) \rightarrow (k_r\rho_s, k_\theta\rho_s)^{GYRO}$

Step 2: Compute derivatives: $\frac{\partial R}{\partial r}(r_{loc},\theta)$

(r_{loc}, θ_{loc}) is location of scattering

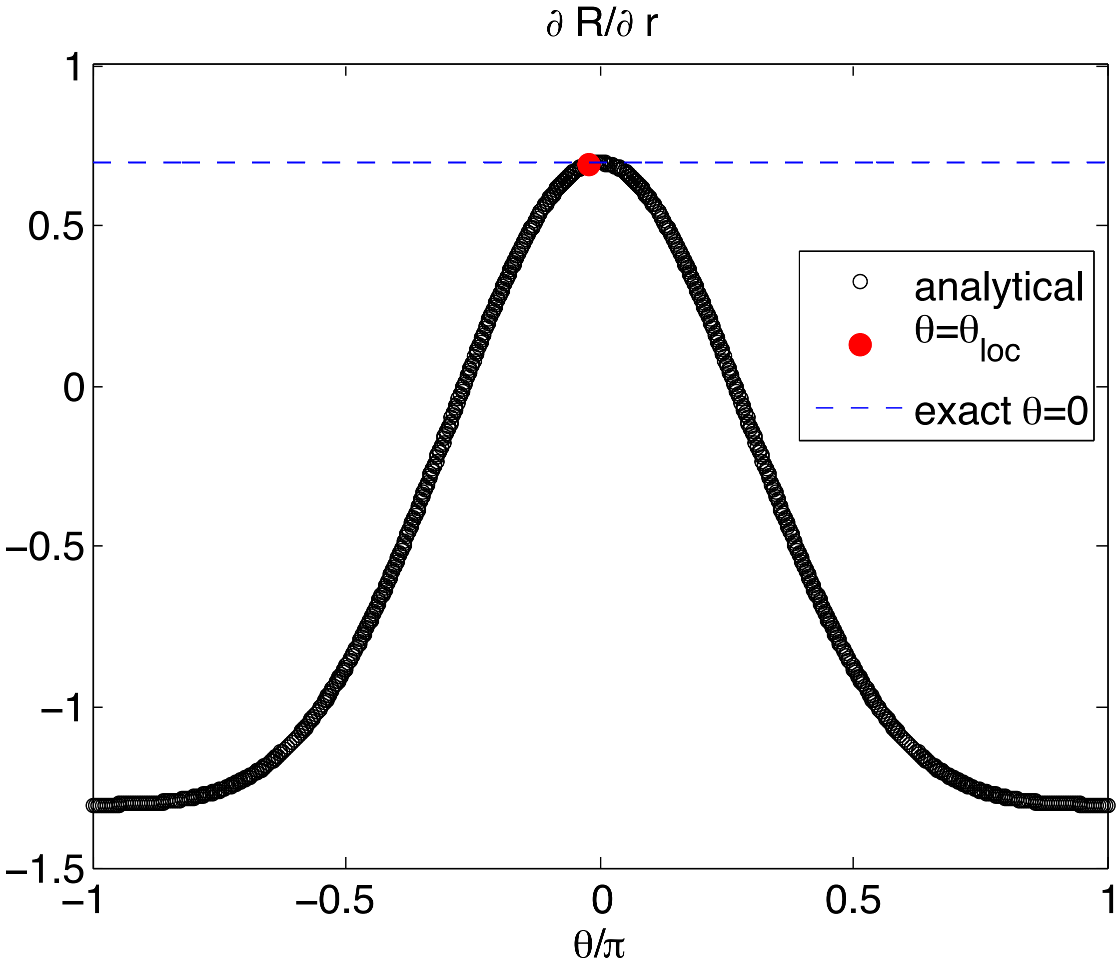

Analytical value at θ=0 is (GS eq

$$\frac{\partial R}{\partial r}(r,\theta=0)=1+\frac{\partial R_0}{\partial r}(r,\theta=0)$$
$$=1+SHIFT$$

37

Inverse Mapping $(k_R, k_Z) \rightarrow (k_r\rho_s, k_\theta\rho_s)^{GYRO}$

Step 2: Compute derivatives: $$\frac{\partial R}{\partial \theta}(r_{loc}, \theta)$$

(r_{loc}, θ_{loc}) is location of scattering

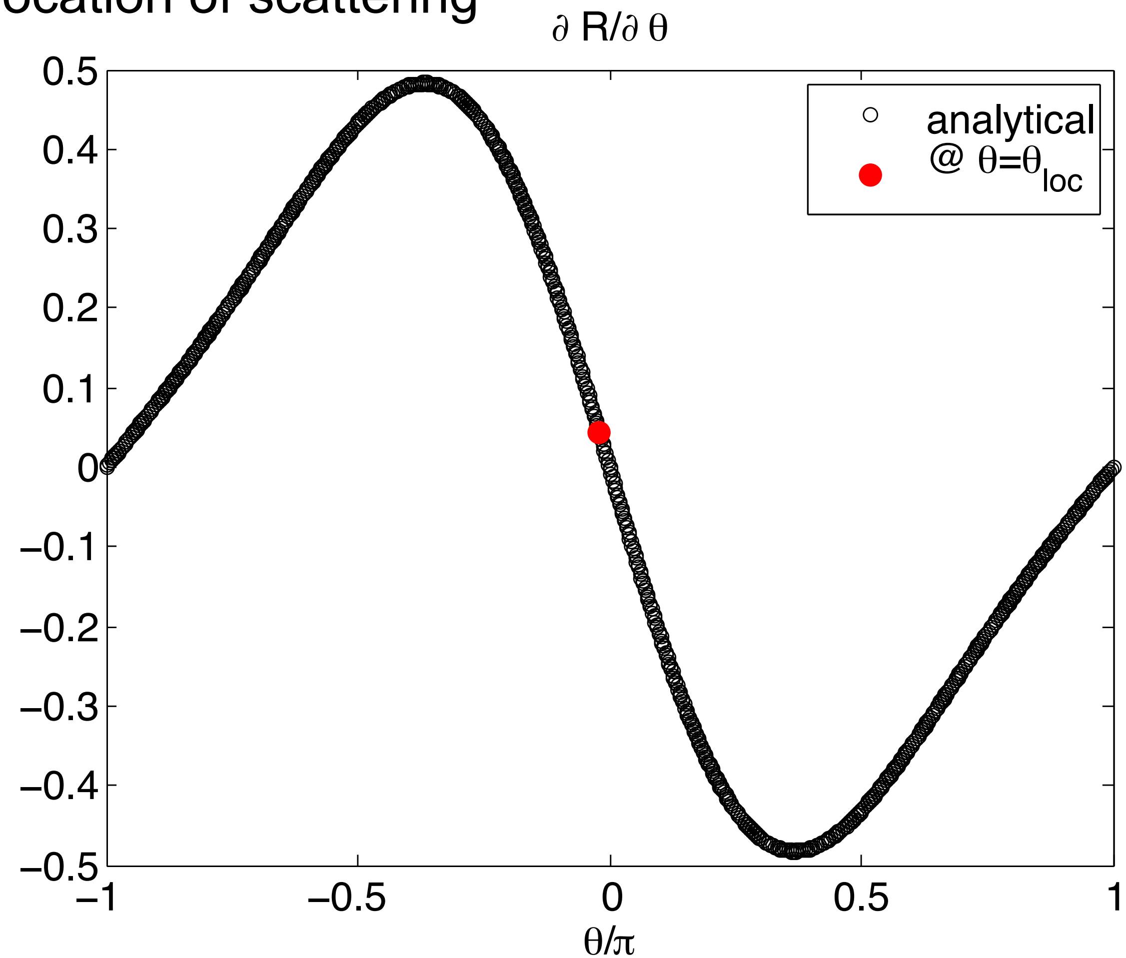

38

Inverse Mapping $(k_R, k_Z) \rightarrow (k_r\rho_s, k_\theta\rho_s)^{GYRO}$

Step 2: Compute derivatives: $\frac{\partial Z}{\partial r}(r_{loc},\theta)$

(r_{loc}, θ_{loc}) is location of scattering

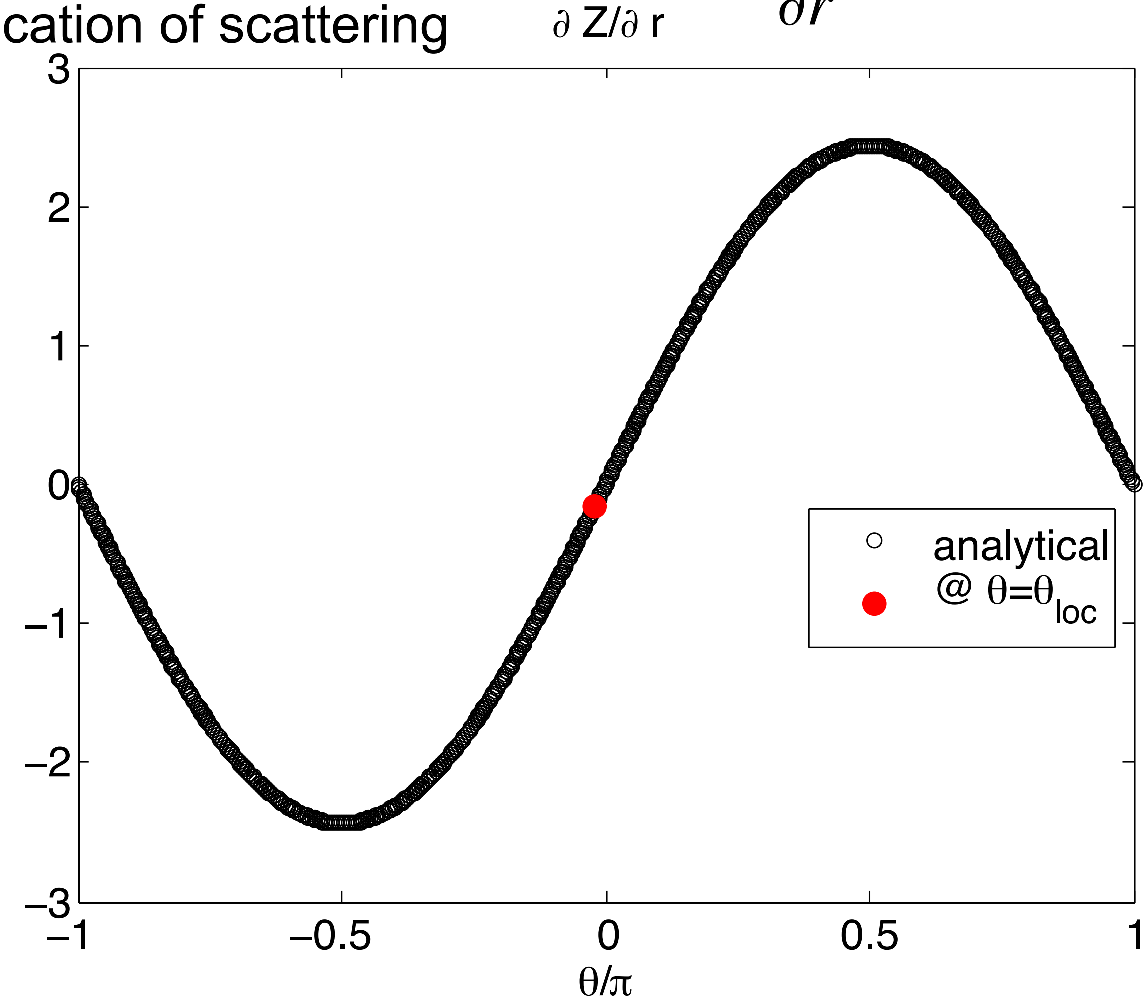

39

Inverse Mapping $(k_R, k_Z) \rightarrow (k_r\rho_s, k_\theta\rho_s)^{GYRO}$

Step 2: Compute derivatives: $\frac{\partial Z}{\partial \theta}(r_{loc}, \theta)$

(r_{loc}, θ_{loc}) is location of scattering

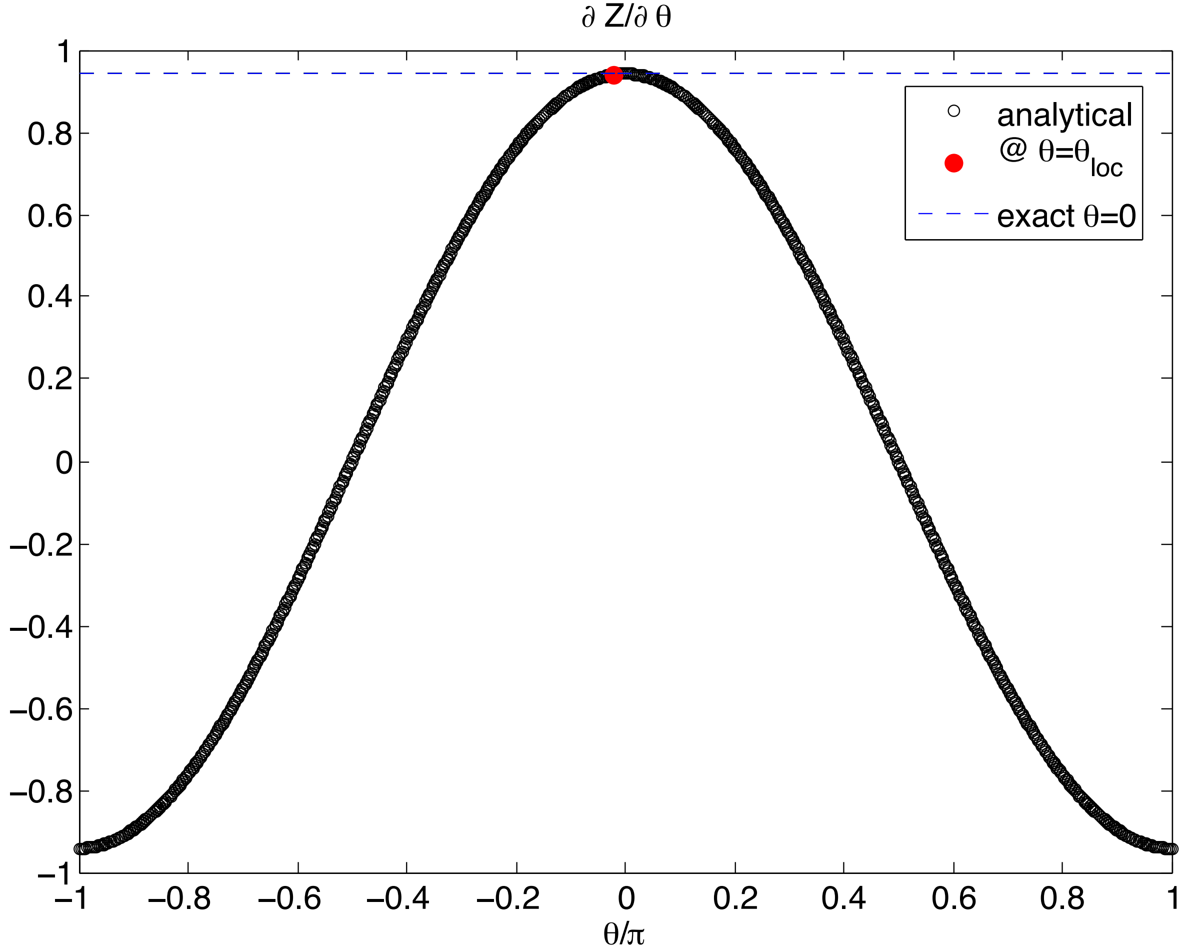

Analytical value at θ=0 is (GS eq

$$\frac{\partial Z}{\partial \theta}(r, \theta = 0) = r\kappa$$

$$= r_{loc} * KAPPA$$

40

Appendix: Compute Inverse Derivatives

Start from the coordinate transformation

$$\begin{pmatrix} \delta R \\ \delta Z \end{pmatrix} = \begin{pmatrix} \frac{\partial R}{\partial r} & \frac{\partial R}{\partial \theta} \\ \frac{\partial Z}{\partial r} & \frac{\partial Z}{\partial \theta} \end{pmatrix} \begin{pmatrix} \delta r \\ \delta \theta \end{pmatrix} = J \begin{pmatrix} \delta r \\ \delta \theta \end{pmatrix} \Leftrightarrow \begin{pmatrix} \delta r \\ \delta \theta \end{pmatrix} = J^{-1} \begin{pmatrix} \delta R \\ \delta Z \end{pmatrix}$$

Additionally, we can write the inverse transformation

$$\begin{pmatrix} \delta r \\ \delta \theta \end{pmatrix} = \begin{pmatrix} \frac{\partial r}{\partial R} & \frac{\partial r}{\partial Z} \\ \frac{\partial \theta}{\partial R} & \frac{\partial \theta}{\partial Z} \end{pmatrix} \begin{pmatrix} \delta R \\ \delta Z \end{pmatrix}$$

Compute inverse matrix J^{-1}

$$J^{-1} = \frac{1}{\det J} \begin{pmatrix} \frac{\partial Z}{\partial \theta} & -\frac{\partial R}{\partial \theta} \\ -\frac{\partial Z}{\partial r} & \frac{\partial R}{\partial r} \end{pmatrix}, \quad \det J = \frac{\partial R}{\partial r}\frac{\partial Z}{\partial \theta} - \frac{\partial R}{\partial \theta}\frac{\partial Z}{\partial r}$$

* Recall dRdθ =0
* Recall dZ/dr =0

Appendix: Compute Inverse Derivatives

We find

$$\begin{cases} \dfrac{\partial r}{\partial R} = \dfrac{1}{\det J}\dfrac{\partial Z}{\partial \theta} \\ \dfrac{\partial r}{\partial Z} = -\dfrac{1}{\det J}\dfrac{\partial R}{\partial \theta} \\ \dfrac{\partial \theta}{\partial R} = -\dfrac{1}{\det J}\dfrac{\partial Z}{\partial r} \\ \dfrac{\partial \theta}{\partial Z} = \dfrac{1}{\det J}\dfrac{\partial R}{\partial r} \end{cases}$$

$$\det J = \frac{\partial R}{\partial r}\frac{\partial Z}{\partial \theta} - \frac{\partial R}{\partial \theta}\frac{\partial Z}{\partial r}$$

Steps:

Compute forward derivatives

Compute inverse derivatives

Complete (k_R, k_Z) mapping

Conclusions and Future Work on Synthetic Diagnostic

- Implement instrumental selectivity function and wavenumber filtering.

- **Goal**: a direct, quantitative comparison between experiment-GYRO simulation of e- scale turbulence.
  - Compare fluctuation spectrum high-k diagnostic/synthetic high-k.
  - Study energy transfer between different k's (different channels).

- Project operating space of new high-k diagnostic.
  - Are streamers predicted to be detected with the new high-k system?

- Study turbulence characteristics in high-resolution e- scale run → towards multiscale simulation in NSTX-U.
  - High-resolution electron scale runs presented here are NOT multiscale
    - Ions are not resolved correctly $\Delta k_\theta \rho_s$~0.3, L_r x L_y = 21 x 21 ρ_s.
    - Simulation ran only for electron time scales (~20a/c_s), ions are not fully developped.
  - In future, can apply synthetic high-k to multiscale simulation in NSTX-U.

This work is supported by US. D.O.E. Contract No. DE-AC02-09CH11466. Computer simulations were carried out at the National Energy Research Scientific Computing Center, US. D.O.E. Contract No. DE-AC02-05CH11231.

Title here

- Column 1
- Column 2

Intro

- First level
  - Second level
    - Third level
      - You really shouldn't use this level – the font is probably too small

Here are the official NSTX-U icons / logos

NSTX Upgrade

NSTX Upgrade

NSTX-U

NSTX-U

National Spherical Torus
eXperiment Upgrade

National Spherical Torus eXperiment Upgrade

Instructions for editing bottom text banner

- Go to View, Slide Master, then select top-most slide
  - Edit the text box (meeting, title, author, date) at the bottom of the page
    - Then close Master View